TOPOLOGICAL ANALYSES OF THE ELECTRONIC DENSITY OF H-NbSe$_2$ COMPLEXES

Alvanh Alem G. Pido
Department of Physics, Mindanao State University – Main Campus 9700 Marawi City, Philippines
alvanhalem.pido@msumain.edu.ph

ABSTRACT

Transition metal dichalcogenides are among the emerging two-dimensional materials nowadays due to their unique and extraordinary properties. Niobium Diselenide (NbSe$_2$) is a transition metal dichalcogenide that has been formed by sandwiching one Nb atom with two Se atoms. In this work, we dope H atoms to 1 x 1 x 1 monolayer NbSe$_2$ and performed topological analyses to find the charge transfer and binding mechanism of the resulting H-NbSe$_2$ complexes. Calculations of the binding energies revealed that the strength of interaction is proportional to H coverages in the system. Further, charge redistributions have been observed in the system. Bader charge analysis reveals that the charge transfer is towards the H atoms with a magnitude of up to 1.13 *e*. Finally, it was revealed that the strength of interaction between the H and NbSe$_2$ depends on where H bonds directly.

Keywords:* *Transition metal dichalcogenides, two-dimensional materials, NbSe$_2$, monolayer, topological analyses, binding energies

INTRODUCTION

The postmodernist leverage of science has motivated many scientists to unravel prevalent technologies that could stipulate our demands. The advancement of two-dimensional materials [1, 3, 12,13] has unleashed a new era for nanoelectronic devices. The discovery of graphene [10, 11] led the search for other two-dimensional materials. Some of the interesting two-dimensional materials nowadays are the transition metal dichalcogenides [7]. These are formed by sandwiching one Transition metal atom with two Chalcogen atoms [12].

Pido, A.A. & Bryan, P. [12] recently studied the Oxygen impurities on monolayer Niobium Diselenide (NbSe$_2$) [6] to investigate how the resulting complexes behave. Calculations of the charge density difference (CDD) [15] and Bader charge analysis [14] revealed that O and O$_2$ served as oxidizing agents when interacting with the monolayer. Nguyen, et.al [9] investigated the atomic defects and impurities in NbSe$_2$ to see how foreign atoms react to defects. Accordingly, these impurities can stabilize the defected monolayer, particularly in the Se divacancies. According to a study by Yeon. K.H., et.al [18], hydrogen adsorption causes a metal to semiconductor transition of NbSe$_2$. However, despite many studies about impurities to NbSe$_2$, the nature of charge transfer and binding mechanism of H-NbSe$_2$ is still not well understood.

In this work, we investigate the interaction of H atoms with different coverages with the monolayer NbSe$_2$ and calculated the magnitude and direction of charge transfer and the binding mechanism of the resulting complexes using the *Ab initio* Density Functional Theory [2] in Quantum Espresso [4] to provide insights about the behaviour of the resulting complexes that could lead to possible practical applications in the future.

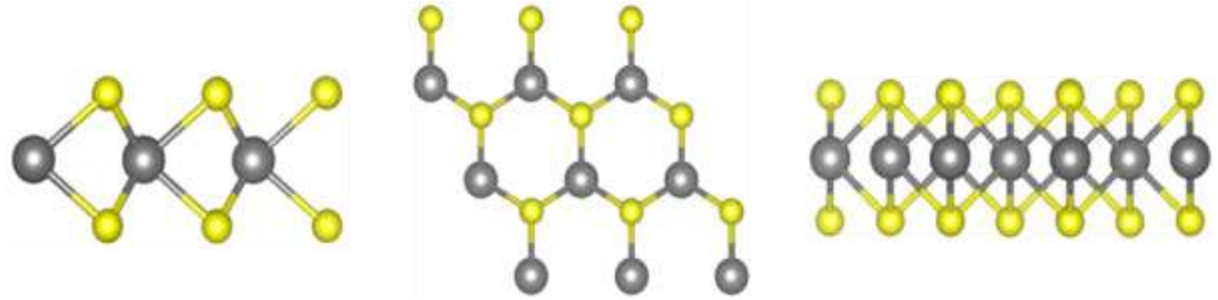

Figure 1. (a) Front, (b) top, and (c) side views of monolayer *2H*-$NbSe_2$. From [12]

COMPUTATIONAL DETAILS

We make use of the *Ab initio* Density Functional Theory in Quantum Espresso [4] for all our calculations. The exchange-correlation was described within the Local Density Approximation (LDA) [16]. All the structures were optimized with a convergence criterion of 10^{-08} au in self-consistent field (SCF) calculation of energy and structure. We allow them to fully relax until the individual ionic forces are less than 1.0 x 10^{-05} eV/au. We used a 1 x 1 x 1 supercell to mimic the $NbSe_2$. Finally, we mesh the reciprocal space at 16 x 16 x 1 using Monkhorste-pack meshes [8].

To avoid the interaction of neighboring monolayers of $NbSe_2$, we introduced a 14 Å vacuum slab with respect to the z-axis. Convergence testing allowed us to set the energy cut-off to 40 Ry. To obtain the stability of our structures, we calculated the binding energies using

$$E_b(pristine) = E_{NbSe_2} - E_{Nb} - 2Se \qquad (1)$$

for the pristine $NbSe_2$ where E_{Nb} and E_{Se} are the energies of the isolated Nb and Se respectively. For the hydrogenated $NbSe_2$, the binding energy is given by

IEJRD
E-ISSN NO:2349-0721

$$E_b(impure) = \frac{E_{H_nSe_2} - E_{NbSe_2} - nE_H}{n} \qquad (2)$$

where E_{HNbSe2} and E_{NbSe2} are the energies of the hydrogenated and pristine $NbSe_2$, E_H is the energy of isolated H atom and n is the number of H.

To find the magnitude and direction of the charge transfer between atoms we calculate the charge density difference (CDD) [15] and Bader charge analysis [14] which includes the identification of critical points where the gradient of the density vanishes, such that,

$$\nabla\rho(r) = \frac{\partial\rho(r)}{\partial x}u_x + \frac{\partial\rho(r)}{\partial y}u_y + \frac{\partial\rho(r)}{\partial z}u_z \qquad (3)$$

For the binding mechanism, we calculate the electron localization function (ELF) which is known to identify the type of interaction of certain nanostructures [5]. The ELF is given by,

$$n(r) = \frac{1}{1+\chi(r)}\,; where\ \chi = \frac{\tau_p(r)}{\tau_h(r)} = \frac{\frac{1}{2}\sum_{i=1}^{N}|\nabla\psi_i(r)|^2 - \frac{1}{8}\frac{|\nabla\rho(r)|}{\rho(r)}}{\frac{3}{10}(3\pi^2)^{\frac{2}{3}}\rho(r)^{\frac{5}{3}}} \qquad (4)$$

RESULTS AND DISCUSSIONS

We considered different doping sites for H on the monolayer $NbSe_2$. In Figure 2, we define $HNbSe_2$ as the system where H is attached to the Nb, $NbHSe_2$ for H attached to Se and $Nb2HSe_2$ for two H atoms attached to the individual Se atoms of the monolayer.

(a) (b) (c)

Figure 2. Optimized H-$NbSe_2$ complexes for (a) $HNbSe_2$, (b) $NbHSe_2$, and (c) $Nb2HSe_2$. Here, n stands for the number of H atoms.

IEJRD

We then calculated the binding energies using equations 1 and 2. Figure 3 shows the proportionality of H coverages to the strength of interaction. As seen in the plot, configuration 3 which describes the $Nb2HSe_2$ is the most stable one.

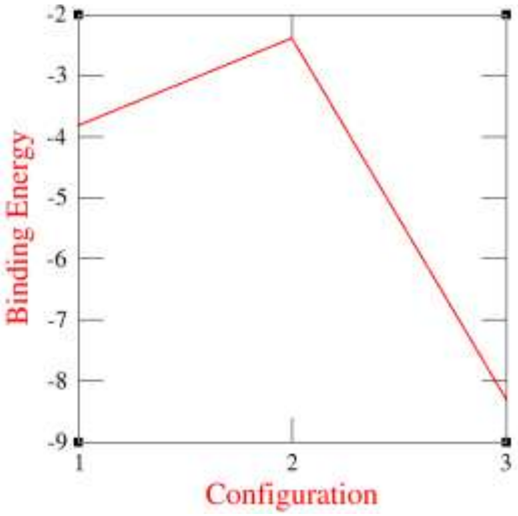

Figure 3. Binding energies of H-$NbSe_2$ complexes.

As shown, the introduction of H to $NbSe_2$ has significantly lowered the binding energy. Table 1 is the tabulated binding energies of the complexes.

Table 1. Binding energies of pristine and doped $NbSe_2$.

Structure	Binding energy (eV)
$NbSe_2$	-10.90
$HNbSe_2$	-3.82
$NbHSe_2$	-2.39
NbH_2Se_2	-8.30

Finally, we performed some topological analyses to investigate the charge transfer and binding mechanism of the complexes. The details are as follows.

Charge Density Difference

Figures 4a to Figure 4c show the CDD of our different configurations for H-doped $NbSe_2$. Charge transfer can be seen all throughout the structures. When one H atom was attached to the Nb atom, we can see that it has both accumulated (yellow) and depleted (cyan) charges. Figure 4b shows that charge accumulation is obvious for the Se-H bond while charge depletion can be seen from the Nb. Figure 4c depicts the charge transfer redistribution in $Nb2HSe_2$. It was revealed that by increasing the H coverage in the $NbSe_2$ by adsorbing H in each of the Se atoms, the charge transfer was almost identical for the two Se-H bonds while charge depletion is still present in the Nb atom.

IEJRD

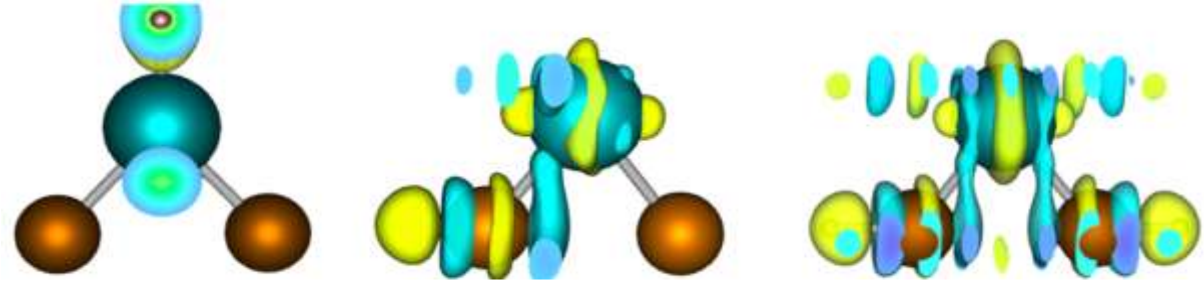

(a) (b) (c)

Figure 4. Charge density difference (CDD) of (a) $HNbSe_2$, (b) $NbHSe_2$, and (c) NbH_2Se_2.

By making use of the Bader charge analysis, we were able to calculate the magnitude and direction of the charges on each atom induced by H-doping. The net charge transfer was calculated by subtracting the Bader charge of pristine $NbSe_2$ and H-$NbSe_2$. The results are shown in the following Tables.

Table 2 shows the Bader charges on each atom of pristine $NbSe_2$ and $HNbSe_2$. We observed that the charges on each atom of the $NbSe_2$ decreased by a magnitude of ~ 0.10 *e* and 0.18 *e* for the Se and Nb respectively, after H-doping. We also calculated the Bader charges of isolated and complex H atoms (complex means the one attached to the monolayer). It was revealed that the isolated H atom has a Bader charge of 1.0 *e*. After doping the monolayer with H, the charge in the complex H increased by ~0.39 *e*.

Table 2. Magnitude of charge transfer for $HNbSe_2$.

Individual Atoms	$NbSe_2$ (*e*)	$HNbSe_2$ (*e*)	Charge Transfer (*e*)
Se1	6.637973	6.533939	-0.10403
Se2	6.634903	6.530415	-0.10449
Nb	11.7272	11.543	-0.1842
H		1.392542	0.392551

We then attached the H atom on one Se atom. Table 3 reveals that the charge redistribution mostly happened in the Se-H bond. Particularly, the Se in the Se-H bond has depleted charges with a magnitude of ~1.28 *e*. This value is quite large as compared to the previous configuration of $HNbSe_2$. This result reveals that charge depletion of Se atom is more obvious when having direct contact with H atom. Further, it was observed that the Nb atom has accumulated ~0.15 *e* while the complex H atom has accumulated ~1.12 *e*.

Table 3. Magnitude of charge transfer for $NbHSe_2$.

Individual Atoms	$NbSe_2$ (e^-)	$NbHSe_2$ (e^-)	Charge Transfer (*e*)
Se1	6.637973	5.3602	-1.277795
Se2	6.634903	6.6402	0.005265
Nb	11.7272	11.877	0.149389
H		2.123	1.123042

Table 3 shows the tabulated magnitude of charge transfer for the $Nb2HSe_2$ complex. Accordingly, the individual Se atoms have depleted ~ 1.23 *e* while the Nb has accumulated 0.20 *e*. It was evident that the complex H atoms have accumulated charges with a magnitude of ~1.13 *e*.

Table 4. Magnitude of charge transfer for $Nb2HSe_2$.

Individual Atoms	$NbSe_2$ (e^-)	$Nb2HSe_2$ (e^-)	Charge Transfer (*e*)
Se1	6.637973	5.4061	-1.231853
Se2	6.634903	5.407	-1.227932
Nb	11.7272	11.928	0.200856
H1		2.1301	1.13007
H2		2.1287	1.128743

In all the configurations considered, we observed that Se atoms have depleted charge while Nb atoms have accumulated charge except for the case where we have an Nb-H bond. In all circumstances, the H atoms served as charge acceptors which could be attributed to the metallic behaviour of $NbSe_2$ [17] that allows it to donate electrons. Thus, this study confirms that H atom accepts electrons when interacting with metals.

Electron Localization Function

As known, ELF values between 0.7 and 1.0 correspond to regions with high probability of localized electrons, indicating a covalent bonding while values lesser than 0.7 correspond to regions of delocalized electrons like in metallic bonds. Figures 5a to Figure 5c show the 2D displays of the ELF of our H-doped NbSe2.

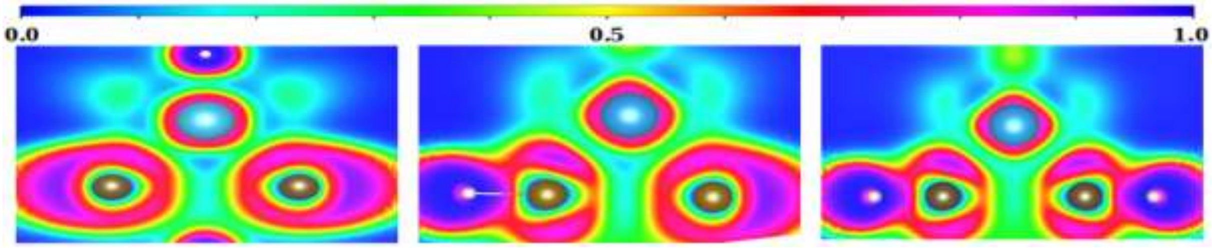

(a) (b) (c)

Figure 5. 2D ELF cuts of (a) $HNbSe_2$, (b) $NbHSe_2$, and (c) NbH_2Se_2 displaying only the regions near the H-$NbSe_2$ interaction where n is the number of H atoms.

It was observed that H atoms have very high probability of localized electrons, consistent with the charge transfer going towards the H atoms as calculated in Bader charge analysis. In Figure 5a, we can see a region of delocalized electrons in the Nb-H bond, though the respective basins of the Nb and H are touching, indicating a weak bonding [5]. In Figure 5b, the Se-H bond shows deep red region of localized electrons revealing a strong interaction between the Se and H. This is consistent with the magnitude of charge transfer in the previous section where the charge accumulated by the H atoms are greater than 1.00 *e* for $NbHSe_2$ and $Nb2HSe_2$ complexes. It is also noted that the strong interaction of Se-H is maintained, regardless of the H coverage.

SUMMARY AND CONCLUSIONS

In this work, we considered the H-doping of 1 x 1 x 1 monolayer $NbSe_2$ and provided a theoretical prediction about the charge transfer and binding mechanism of the resulting complexes. We considered three optimized configurations for our materials, particularly, $HNbSe_2$, $NbHSe_2$ and $Nb2HSe_2$. Among these configurations, $Nb2HSe_2$ is the most stable. It was revealed in the CDD that H doping of the monolayer causes major charge redistributions. Bader charge analysis revealed that Se atoms serve as charge donors while H atoms as charge acceptors.

Further calculations showed that the strength of interaction between the H and $NbSe_2$ depends on where H bonds directly. This is consistent with the findings in the Bader charge analysis where the charge accumulated by H for the Nb-H bond is less than 1.00 *e* while greater than 1.00 *e* for Se-H bonds. These findings may serve as future reference for some electronic properties calculations of nanostructures.

REFERENCES

[1] Alvanh Alem G. Pido. (2022). ENERGY BARRIERS OF N2 ADSORPTION ON SiNR USING NUDGED ELASTIC BAND METHOD. *International Engineering Journal For Research & Development*, *7*(1), 9. https://doi.org/10.17605/OSF.IO/F8B2C.

[2] Bartlett, R. J., Lotrich, V. F., & Schweigert, I. V. (2005). Ab initio density functional theory: The best of both worlds?. *The Journal of chemical physics*, *123*(6), 062205.

[3] Das, S., Robinson, J. A., Dubey, M., Terrones, H., & Terrones, M. (2015). Beyond graphene: progress in novel two-dimensional materials and van der Waals solids. *Annual Review of Materials Research*, *45*, 1-27.

[4] Giannozzi, P., Baroni, S., Bonini, N., Calandra, M., Car, R., Cavazzoni, C., ... & Wentzcovitch, R. M. (2009). QUANTUM ESPRESSO: a modular and open-source software project for quantum simulations of materials. *Journal of physics: Condensed matter*, *21*(39), 395502.

[5] Koumpouras, K., & Larsson, J. A. (2020). Distinguishing between chemical bonding and physical binding using electron localization function (ELF). *Journal of Physics: Condensed Matter*, *32*(31), 315502.

[6] Lawlor, S. D. (2018). *An Investigation Into Niobium Diselenide: Atomic Defects and 2D Properties* (Doctoral dissertation, The University of Manchester (United Kingdom)).

[7] Manzeli, S., Ovchinnikov, D., Pasquier, D., Yazyev, O. V., & Kis, A. (2017). 2D transition metal dichalcogenides. *Nature Reviews Materials*, *2*(8), 1-15.

[8] Monkhorst, H. J., & Pack, J. D. (1976). Special points for Brillouin-zone integrations. *Physical review B*, *13*(12), 5188.

[9] Nguyen, L., Komsa, H. P., Khestanova, E., Kashtiban, R. J., Peters, J. J., Lawlor, S., ... & Haigh, S. J. (2017). Atomic defects and doping of monolayer NbSe2. *ACS nano*, *11*(3), 2894-2904.

[10] Novoselov, K. S., Andreeva, D. V., Ren, W., & Shan, G. (2019). Graphene and other two-dimensional materials. *Frontiers of Physics*, *14*(1), 1-4.

[11] Novoselov, K. S., Morozov, S. V., Mohinddin, T. M. G., Ponomarenko, L. A., Elias, D. C., Yang, R., ... & Geim, A. K. (2007). Electronic properties of graphene. *physica status solidi (b)*, *244*(11), 4106-4111.

[12] Pido, A. A. G., & Pagcaliwagan, B. P. (2022). First principles calculations of the electronic properties of O- and O2-NbSe2 complexes. *International Journal of Computing Sciences Research*, *6*.

[13] Ren, Y., Qiao, Z., & Niu, Q. (2016). Topological phases in two-dimensional materials: a review. *Reports on Progress in Physics*, *79*(6), 066501.

[14] Tang, W., Chill, S., & Henkelman, G. (1970). Bader charge analysis.

[15] Tozini, D., Forti, M., Gargano, P., Alonso, P. R., & Rubiolo, G. H. (2015). Charge difference calculation in Fe/Fe3O4 interfaces from DFT results. *Procedia Materials Science*, *9*, 612-618.

[16] Wills, A. E. (2015). *What Density Functional Theory could do for Quantum Information* (No. SAND2015-1460C). Sandia National Lab.(SNL-NM), Albuquerque, NM (United States).

[17] Xi, X., Zhao, L., Wang, Z., Berger, H., Forró, L., Shan, J., & Mak, K. F. (2015). Strongly enhanced charge-density-wave order in monolayer NbSe 2. *Nature nanotechnology*, *10*(9), 765-769.

[18] Yeoh, K. H., Chew, K. H., Yoon, T. L., Rusi, Chang, Y. H. R., & Ong, D. S. (2020). Metal to semiconductor transition of two-dimensional NbSe2 through hydrogen adsorption: A first-principles study. *Journal of Applied Physics*, *128*(10), 105301 [4] Author1 and Author 2, *Title of Book*, Publisher, Year.

E-ISSN NO:2349-0721